ISSN 1674-1056
http://cpb.iphy.ac.cn
http://iopscience.iop.org/cpb
中国物理 B
Chinese Physics
中国物理 Chinese Physics B

Depolarization field in relaxor-based ferroelectric single crystals under one-cycle bipolar pulse drive

Chuan-Wen Chen, Yang Xiang, Li-Guo Tang, Lian Cui, Bao-Qing Lin, Wei-Dong Du, Wen-Wu Cao
Citation: Chin. Phys. B. 2019, 28 (**12**): 127702 **doi:** 10.1088/1674-1056/ab4e85
Journal homepage: http://cpb.iphy.ac.cn; http://iopscience.iop.org/cpb

What follows is a list of articles you may be interested in

Dielectric and piezoelectric properties of (110) oriented $Pb(Zr_{1-x}Ti_x)O_3$ thin films

Jian-Hua Qiu(邱建华), Zhi-Hui Chen(陈智慧), Xiu-Qin Wang(王秀琴), Ning-Yi Yuan(袁宁一), Jian-Ning Ding(丁建宁)
Chin. Phys. B . 2016, 25(5): 057701 . **doi:** 10.1088/1674-1056/25/5/057701

First-principles study of the relaxor ferroelectricity of $Ba(Zr, Ti)O_3$

Yang Li-Juan, Wu Ling-Zhi, Dong Shuai
Chin. Phys. B . 2015, 24(12): 127702 . **doi:** 10.1088/1674-1056/24/12/127702

Transport properties and anomalous fatigue effect of $Ag/Bi_{0.9}La_{0.1}FeO_3/La_{0.7}Sr_{0.3}MnO_3$ heterostructures

Gao Rong-Li, Fu Chun-Lin, Cai Wei, Chen Gang, Deng Xiao-Ling, Yang Huai-Wen, Sun Ji-Rong, Shen Bao-Gen
Chin. Phys. B . 2014, 23(9): 097702 . **doi:** 10.1088/1674-1056/23/9/097702

Composition and misfit strain dependence of electrocaloric effect of $Pb_{1-x}Sr_xTiO_3$ thin films

Qiu Jian-Hua, Ding Jian-Ning, Yuan Ning-Yi, Wang Xiu-Qin
Chin. Phys. B . 2013, 22(1): 017701 . **doi:** 10.1088/1674-1056/22/1/017701

Effect of misfit strain on the electrocaloric effect of polydomain epitaxial ferroelectric thin films

Qiu Jian-Hua, Ding Jian-Ning, Yuan Ning-Yi, Wang Xiu-Qin
Chin. Phys. B . 2012, 21(9): 097701 . **doi:** 10.1088/1674-1056/21/9/097701

Depolarization field in relaxor-based ferroelectric single crystals under one-cycle bipolar pulse drive*

Chuan-Wen Chen(陈传文)[1,2], Yang Xiang(项阳)[1,†], Li-Guo Tang(汤立国)[3,4], Lian Cui(崔莲)[2,5], Bao-Qing Lin(林宝卿)[1], Wei-Dong Du(杜伟东)[6,‡], and Wen-Wu Cao(曹文武)[2]

[1] *Fujian Provincial Key Laboratory of Light Propagation and Transformation, College of Information Science and Engineering, Huaqiao University, Xiamen* 361021, *China*

[2] *Department of Mathematics and Materials Research Institute, The Pennsylvania State University, University Park, Pennsylvania* 16802, *USA*

[3] *Department of Applied Marine Physics & Engineering, Xiamen University, Xiamen* 361010, *China*

[4] *State Key Laboratory of Acoustics, Institute of Acoustics, Chinese Academy of Sciences, Beijing* 100190, *China*

[5] *School of Electronic and Information Engineering, Yangtze Normal University, Chongqing* 408003, *China*

[6] *Acoustic Science and Technology Laboratory, Harbin Engineering University, Harbin* 150001, *China*

(Received 25 July 2019; revised manuscript received 12 October 2019; published online 22 November 2019)

The $[001]_c$-polarized $(1-x)Pb(Mg_{1/3}Nb_{2/3})O_3$–$xPbTiO_3$ (PMN−PT) single crystals are widely used in ultrasonic detection transducers and underwater acoustic sensors. However, the relatively small coercive field (~ 2 kV/cm) of such crystals restricts their application at high frequencies because the driving field will exceed the coercive field. The depolarization field can be considerably larger in an antiparallel direction than in a parallel direction with respect to polarization when the bipolar driving cycle starts. Thus, if the direction of the sine wave signal in the first half cycle is opposite to the polarization direction, then the depolarized domains can be repolarized in the second half of the sine cycle. However, if the direction of the sine wave signal in the first half of the cycle is along the polarization direction, then the change is negligible, and the domains switched in the second half of the sine cycle cannot be recovered. The design of electric driving method needs to allow the use of a large applied field to emit strong enough signals and produce good images. This phenomenon combined with the coercive field increases with the driving frequency, thereby making the PMN−PT single crystals usable for high-frequency applications. As such, the applied field can be considerably larger than the conventionally defined coercive field.

Keywords: piezoelectric crystal, coercive field, depolarization field, bipolar pulse

PACS: 77.22.Ej, 77.80.Fm, 77.80.Dj, 77.84.Cg **DOI:** 10.1088/1674-1056/ab4e85

1. Introduction

Piezoelectric ceramics and single crystals are important functional materials, which are being used in many electromechanical devices, such as sensors, actuators, transducers, and ultrasonic motors. In recent years, relaxor-based lead magnesium niobate−lead titanate, $(1-x)Pb(Mg_{1/3}Nb_{2/3})O_3$–$xPbTiO_3$, (PMN−PT) single crystals have attracted considerable attention because of their superior piezoelectric properties for compositions near the morphotropic phase boundary.[1–7] When PMN−PT single crystals are poled along the $[001]_c$ of the pseudo-cubic structure, the piezoelectric coefficient d_{33} value can exceed 2500 pC/N, and the electromechanical coupling coefficient k_{33} is greater than 90%.[8]

The coercive field of ferroelectric materials reflects the onset of domain reversal, which is a critical parameter for the application of ferroelectric materials because it indicates the upper limit of the applied field.[9,10] The coercive field of PMN−PT single crystals is considerably lower (1.8 kV/cm–2.5 kV/cm) than that of $Pb(Zr_xTi_{1-x})O_3$ piezoceramics (over 10 kV/cm). This finding greatly restricts the applications of PMN−PT crystals in terms of the driving field level. Moreover, the crystal is only partially depolarized, rendering it unusable in practical applications. We call this effective coercive field E_{ec}, which is smaller than the conventionally defined coercive field E_c.[11] Several methods can be used to increase the coercive field of ferroelectric materials. One method is to increase the applied field frequency because the coercive field increases with frequency.[12–14] The coercive field is defined at very low frequencies (< 1 Hz). In ultrasonic transducers, the center frequency is much higher, rendering E_{ec} higher than E_c. Another method is to apply a bias field along the polarization direction.[15] The coercive field can also be enhanced via doping the acceptor ions, which introduces an internal bias.[16–19]

In this work, we describe a different strategy to increase

*Project supported by the National Natural Science Foundation of China (Grant No. 11674270), the Fundamental Research Funds for Xiamen University, China (Grant No. 20720180113), the Education and Scientific Research Project for Young and Middle-aged Teachers of Fujian Province, China (Grant No. JAT170036), the Opening Fund of Acoustics Science and Technology Laboratory, China (Grant No. SSKF2018006), and one of the authors, Chuan-Wen Chen, was sponsored by the Education Department of Fujian Province, China for his study at the Pennsylvania State University (Grant No. 2016071145).

†Corresponding author. E-mail: yxiang@hqu.edu.cn

‡Corresponding author. E-mail: duweidong@hrbeu.edu.cn

© 2019 Chinese Physical Society and IOP Publishing Ltd

the effective coercive field in a bipolar drive situation. The method of applying this bipolar pulse electric field has a remarkable effect on the degradation of ferroelectric properties. In an antiparallel situation (Fig. 1(a)), the direction of the applied electric field is opposite to the remnant polarization direction of the sample in the first half period. In the second half period, the field is along the polarization direction. The parallel situation turns opposite as shown in Fig. 1(b). Only one-cycle signal is used in our experiments.

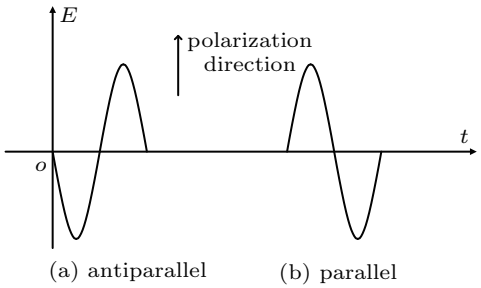


Fig. 1. Schematic diagram of two methods of applying bipolar electric field.

2. Experiments

The $[001]_c$-polarized PMN–0.30 PT single crystal plates with gold electrodes are made by CTS Inc., USA. The samples were cut into small plates and polished. Their final sizes were about 2.5 mm (L) ×2.5 mm (W) ×0.289 mm (T). The coercive field E_c was 1.68 kV/cm, remnant polarization was 0.21 C/m^2 based on the loop measured at 0.1 Hz, and the piezoelectric constant d_{33} was 1318 pC/N. The effects of the initial direction of the bipolar signal on sample depolarization were studied at low and high frequencies. In the low-frequency experiments, the ferroelectric hysteresis loops were measured between 0.01 Hz and 500 Hz by using a modified Sawyer Tower circuit. The electric field between 0.03 kV/cm and 4.84 kV/cm with a sinusoidal bipolar waveform was generated by a high voltage amplifier (Trek Model 2210). In the high-frequency experiments, sinusoidal pulse signals with frequencies of 100 kHz, 200 kHz, 300 kHz, and 400 kHz were generated by a pulse/function generator (Wavetek Model 81), respectively. Then, each of the signals was amplified up to 15 kV/cm by using an RF broadband power amplifier (Electronics & Innovation 1040 L). The burst signal was monitored by a digital oscilloscope (Tektronix TDS 680C). The electromechanical coupling factor k_t was measured by using an impedance analyzer (HP 4194 A).

Only one-cycle of the sinusoidal bipolar waveform was applied in the low- and high-frequency experiments. On the basis of the method through which the electric pulse was applied, the test was divided into two groups, namely, parallel and antiparallel, as shown in Fig. 1.

3. Results and discussion

After the application of one cycle of a sine wave electric pulses of varying amplitudes, the hysteresis loop for parallel and antiparallel situations are determined, as shown in Figs. 2(a) and 2(b), respectively. If the applied electric field is weak, then the depolarization of the sample is negligible. Polarization changes almost linearly with the applied electric field near the remnant polarization point. However, when the applied electric field is sufficiently high, a nonlinear behavior is observed for parallel and antiparallel situation.

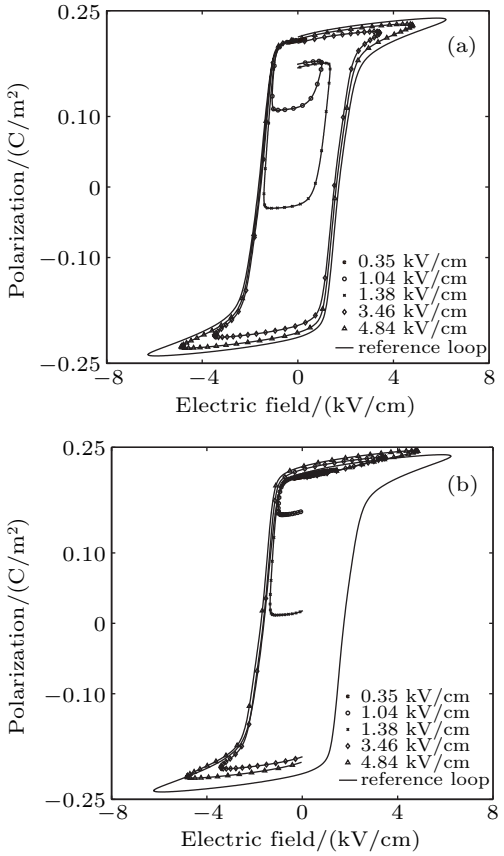


Fig. 2. Hysteresis loops under 0.1-Hz electrical signal with only one-cycle when field starts in direction (a) antiparallel and (b) parallel to the polarization direction.

For an antiparallel situation (Fig. 2(a)), polarization decreases evidently as the electric field amplitude increases to its negative maximum value when the applied electric field is strong enough. Some domains are reversed, become partially depolarized in the first half period, which is marked as depolarization (*i.e.*, $a' \rightarrow b' \rightarrow c'$ in Fig. 3). In the second half period, the electric field is switched into the same direction as that of polarization, and most of the reversed domains are switched back to their original poled state. The remnant polarization is almost recovered to its original state. Thus, the crystal is not depolarized after a full bipolar cycle. The second half cycle is a polarization process (*i.e.*, $c' \rightarrow d' \rightarrow e'$ in Fig. 3). The polarized state is a metastable state, and the sample can be depolarized by a field smaller than its coercive field. However, fully

polarizing the sample is difficult. The external field is usually more than twice its coercive field. As a result, depolarization has a greater effect on the polarization state of the sample than polarization. If only one-cycle bipolar signal is applied, the final polarization P_f (*i.e.*, the polarization at points e' or e as shown in Fig. 3) will decrease slightly as shown in Fig. 2(a). When the electric field becomes large enough but still smaller than the coercive field, the sample is largely depolarized and unusable.

The parallel starting field direction situation comprises two processes, namely, enhanced polarization and depolarization. The first half period is for the enhanced polarization, and the second half period is for the depolarization. In the enhanced polarization (*i.e.*, $a \to b \to c$ in Fig. 3), polarization increases slightly. In the second half of the signal, which is for depolarization (*i.e.*, $c \to d \to e$ in Fig. 3), the depolarization in the sample is clear and similar to the scenario in the first half cycle in the antiparallel situation. If the applied field strengthens, this depolarization effect also increases. Finally, polarization is completely reversed as shown in Fig. 2(b).

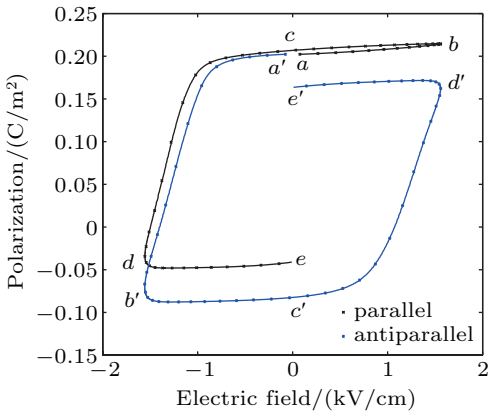


Fig. 3. Comparison between hysteresis loops for parallel and antiparallel situations under a one-cycle bipolar electrical pulse with amplitude of 1.56 kV/cm.

Figure 3 shows the hysteresis loops under 1.56 kV/cm for the parallel and antiparallel situation. After the application of one-cycle signal, the final polarization P_f of the antiparallel situation (polarization at point e') is remarkably larger than that of the parallel situation (polarization at point e). In a parallel situation, enhanced polarization $a \to b \to c$ occurs in the first half cycle. Given that the sample is already in the saturation polarization state, this process has a negligible effect on the polarization state of the sample. In theory, if a sample is in the saturation polarization state, polarization cannot increase; thus, the first enhanced polarization in the parallel situation has a limited effect on remnant polarization. In the second half of the pulse cycle ($c \to d \to e$ in Fig. 3), the sample is depolarized, which is similar to the first half cycle situation for the antiparallel situation ($a' \to b' \to c'$ in Fig. 3). However, the final polarization P_f for antiparallel situation should be larger than that in the parallel situation after the bipolar cycle, because it exhibits polarization after depolarization. Experimental results show that the enhanced polarization in the parallel situation ($a \to b \to c$ in Fig. 3) can increase the polarization of the crystal (Fig. 3). In Fig. 4, the hysteresis loops are under 3.46 kV/cm and 4.84 kV/cm. The difference in remnant polarization (ΔP_r) between the two loops is only 0.01 C/m^2. However, when the electric field decreases to -1.5 kV/cm, the polarization difference in polarization between the two loops increases to 0.028 C/m^2 ($\Delta P = 0.025$ C/m^2 at $+1.5$ kV/cm), which is 2.8 times the value of ΔP_r. The closer to the rectangle shape the hysteresis loop, the greater the difference between ΔP and ΔP_r will be.

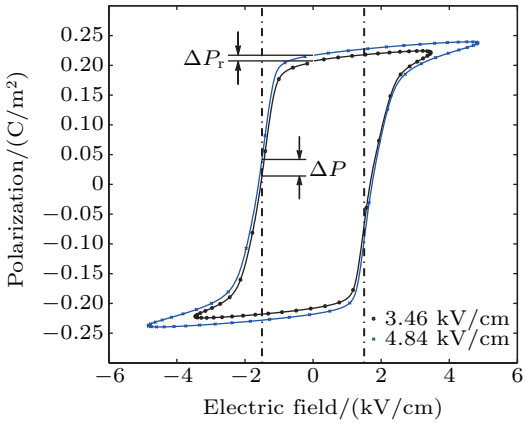


Fig. 4. Hysteresis loops under different electric fields.

Figure 5 shows the variation of the final polarization P_f with the applied electric field at 0.1 Hz and 100 Hz after a one-cycle bipolar electric pulse. The variation for 0.1-Hz case and 100-Hz case show a similar trend. In the parallel situation, the sample is gradually depolarized with the increase of the applied electric field amplitude and is polarized in the opposite direction. When the electric field is sufficiently strong (over 1.42 kV/cm in 0.1 Hz and over 2.12 kV/cm in 100 Hz), depolarization can completely depolarize the sample and polarize the sample in the opposite direction. However, in the antiparallel case, P_f gradually decreases to a minimum value with the increasing of applied electric field and returns to its saturated polarization state at 0.1 Hz. The antiparallel state exhibits the polarization state after depolarization in comparison with the parallel state. This polarization process can recover most of the lost polarizations. However, the decreasing of P_f in the 100-Hz case is not significant (Fig. 5(b)). At high electric field frequency, the electric field has a short action time on polarization. Thus, the effect of polarization and depolarization on the domains are low. This phenomenon caused the value of P_f to vary less with the electric field increasing as shown in Fig. 5(b). The method through which the electric field is

applied has a considerable effect on the polarization status of a sample and determines the maximum field that it can withstand.

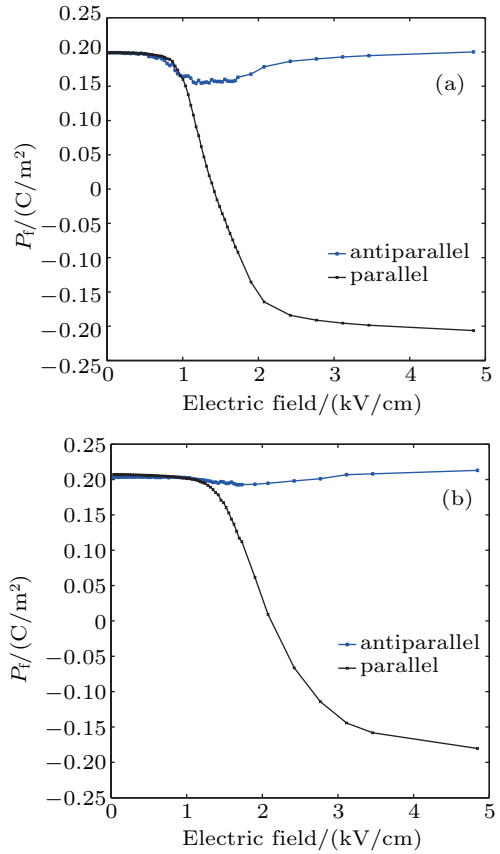


Fig. 5. Variations of final polarization with electric field of a bipolar pulse at (a) 0.1 Hz and (b) 100 Hz.

Depolarizations at high frequencies are also studied. In contrast to the work of Li *et al.*, where a burst signal with two or more cycles of a sine wave was triggered by a 4-MHz pulse,[20] here in this work we only use a one-cycle sine wave signal in the high-frequency impedance test. The samples are divided into two groups, namely, parallel and antiparallel situations. The variations of the impedance spectrum under different external fields are studied for these two situations. The sample's depolarization state can be judged by changing the electromechanical coupling coefficient k_t, which can be calculated by the resonant frequency f_r and anti-resonant frequency f_a from the following formula:

$$k_t = \left(\frac{\pi}{2}\frac{f_r}{f_a}\tan\left(\frac{\pi}{2}\frac{f_a - f_r}{f_a}\right)\right)^{1/2}. \quad (1)$$

The signals with 100 kHz, 200 kHz, 300 kHz, and 400 kHz are used in high-frequency testing. Polarization reversal of the sample occurs only when the bipolar electric field reaches a critical level. Moreover, the critical field in the antiparallel case is considerably greater than in the parallel case. The critical level increases with frequency increasing. In the antiparallel situation, when the frequency is greater than 200 kHz, and the sinusoidal pulse reaches 15 kV/cm, no depolarization is observed or the sample is damaged before depolarization. When the field reaches 15 kV/cm, depolarization does not occur above 200 kHz. The polarization decreases rapidly after a certain value in the parallel and the antiparallel case. An effective coercive field E_{ec} is defined as the corresponding electric field value at which the relevant parameter (polarization at low frequency and k_t at high frequency) drops to 80% of the original value. We denote E_{ec} as E_{ec}^{P} in the parallel situation and E_{ec}^{A} in the antiparallel situation to distinguish between the parallel and the antiparallel situations. The effective coercive fields for the low- and high-frequency test are listed in Table 1. In the case of 100 kHz, the maximum decrease of the antiparallel case is only 5.7%. The corresponding electric field is defined as the effective coercive field E_{ec}^{A}.

E_{ec}^{A} is greater than E_{ec}^{P}, and their difference becomes larger with frequency increasing. As shown in Table 1, E_{ec}^{P} and E_{ec}^{A} become large as the test frequency increases. Our test setup cannot measure the coercive field at a test frequency higher than 200 kHz. Only one cycle of sine pulse is applied; thus, the results are different from previous investigations in which repeated one cycle pulse was applied.[9] Also, E_{ec}^{P} and E_{ec}^{A} substantially decrease. However, E_{ec}^{A} is still considerably greater than E_{ec}^{P}.

Table 1. Effective coercive fields under different test frequencies.

	E_{ec}^{P}/(kV/cm)	E_{ec}^{A}/(kV/cm)
0.1 Hz	1.01	1.14
100 Hz	1.50	1.70
100 kHz	5.49	12.14

This phenomenon can be explained by domain switching. The switching of the polarization has a relaxation time τ, which is field-dependent and expressed as[21]

$$\tau = \tau_0 \exp(-E_0/E_t), \quad (2)$$

where τ is a characteristic relaxation time, τ_0 is a constant, E_0 is an activation field, and E_t is the total field, which is the sum of the applied field E and the random field.

This relaxation time decreases rapidly with the electric field but does not change considerably with measurement frequency within a certain frequency range.[11] In the $[001]_c$-poled rhombohedral PMN–0.30 PT single crystals, 109°, 71°, and 180° domain switching processes are involved when the sample is polarized or depolarized.[22,23] The switching time of non-180° domains is longer than that of 180° domains. As a result, the non-180° domains at high frequencies cannot follow the field change. Hence, switching the polarization under high-frequency electric field is difficult. An extensive field strength is needed for the high-frequency field to depolarize

the sample to the same level. As such, the sample has a relatively large coercive field at high measurement frequency.

In summary, we investigate the effects of different methods applied to the electric field on the effective coercive field of $[001]_c$-poled $0.70Pb(Mg_{1/3}Nb_{2/3})O_3$–$0.30PbTiO_3$ single crystal by combining the hysteresis loop measurements and the impedance spectroscopy measurements. Only a single one-cycle sinusoidal electric pulse is applied. The test groups are divided into parallel and antiparallel group with respect to the polarization on the basis of the method through which the electric field is applied. The one-cycle signal can be divided into two half cycle processes, *i.e.*, enhanced polarization and depolarization. In a parallel situation, the first is to enhance the polarization followed by depolarization, whereas the opposite sequence follows in an antiparallel situation. In a parallel case, the first enhanced polarization only slightly increases the polarization as the sample is already fully polarized. In the second half of the cycle, *i.e.*, in the depolarization process, the sample is partially depolarized is a sufficiently large field. In the antiparallel case, the sample is initially depolarized first during depolarization and repolarized by the enhanced polarization. Thus, P_f in the antiparallel case is larger than that in the parallel case. This phenomenon has an extreme case as follows. When the field is beyond the coercive field, the sample is repolarized into an original polarization state in the antiparallel case and polarized in the opposite direction in the parallel case. Thus, the two methods of applying a large electric field have considerably different consequences. With the increasing of test frequency, the effective coercive fields E_{ec}^{P} and E_{ec}^{A} are extensive, and their differenceis remarkable. Our results might serve as useful guide for designing electrical driving circuits that use PMN−PT single crystal probes in underwater acoustic engineering.

References

[1] Wang R, Xu H, Yang B, Luo Z, Sun E, Zhao J, Zheng L, Dong Y, Zhou H, Ren Y, Gao C and Cao W 2016 *Appl. Phys. Lett.* **108** 152905
[2] Chen Y, Zhang Y, Zhang L, Ding F and Schmidt O G 2017 *Nano Energy* **31** 239
[3] Wang C, Liu Y, Zhang R, Yang B and Cao W 2017 *J. Alloys Compd.* **699** 442
[4] Wang D, Yuan G L, Luo H S, Li J F, Viehl D and Wang Y J 2017 *J. Am. Ceram. Soc.* **100** 4938
[5] Matsuura M, Koreeda A, Kim T H and Han Y S 2017 *Ferroelectrics* **513** 27
[6] Qiu J H, Wang X Q, Yuan N Y and Ding J N 2015 *Chin. Phys. B* **24** 077701
[7] Li X J, Fan X, Xi Z Z, Liu P, Long W, Fang P Y and Nan R H 2019 *Chin. Phys. B* **28** 57701
[8] Zhang R, Jiang B and Cao W W 2001 *J. Appl. Phys.* **90** 3471
[9] Ge W, Zeng H, Shuai Y and Zhang W 2019 *Mater. Res. Express* **6** 035033
[10] Morozovska A N, Eliseev E A, Vorotiahin I S, Silibin M V, Kalinin S V and Morozovsky N V 2018 *Acta Mater.* **160** 57
[11] Chen Z, Zhang Y, Li S, Lu X M and Cao W 2017 *Appl. Phys. Lett.* **110** 202904
[12] Yin J and Cao W 2002 *Appl. Phys. Lett.* **80** 1043
[13] Chen X, Dong X, Zhang H, Cao F, Wang G, Gu Y, He H, Liu Y and Li W 2011 *J. Am. Ceram. Soc.* **94** 4165
[14] Su Y, Liu N and Weng G J 2015 *Acta Mater.* **87** 293
[15] Wilkie W K, Inman D J, Lloyd J M and High J W 2016 *J. Intell. Mater. Syst. Struct.* **17** 15
[16] Yang L, Zheng L, Jing Y, Li S, Lu X, Lü W and Zhang R 2017 *Phys. Status Solidi B* **254** 1700029
[17] Zheng L, Sahul R, Zhang S, Jiang W, Li S and Cao W 2013 *J. Appl. Phys.* **114** 104105
[18] Zheng L, Yang L, Li Y, Lu X, Huo D, Lü W, Zhang R, Yang B and Cao W 2018 *Phys. Rev. Appl.* **9** 064028
[19] Luo N, Zhang S, Li Q, Yan Q, Zhang Y, Ansell T, Luo J and Shrout T R 2016 *J. Mater. Chem. C* **4** 4568
[20] Li S, Chen Z and Cao W 2016 *Appl. Phys. Lett.* **108** 232901
[21] Viehl D and Chen Y H 2000 *J. Appl. Phys.* **88** 6696
[22] Erhart J and Cao W 2012 *Ferroelectrics* **426** 13
[23] Yin J H and Cao W W 2000 *J. Appl. Phys.* **87** 7438